Pseudospectra and delay differential equations

Kirk Green [1] Thomas Wagenknecht [2]

Abstract

In this paper we present a new method for computing the pseudospectra of delay differential equations (DDEs) with fixed finite delay. This provides information on the sensitivity of eigenvalues under arbitrary perturbations of a given size, and hence insight into how stability may change under variation of parameters. We also investigate how different weighted perturbations applied to the individual matrices of the delayed eigenvalue problem affect the pseudospectrum. Furthermore, we compute pseudospectra of the infinitesimal generator of the DDE, from which a lower bounds on the maximum transient growth can be inferred. To illustrate our method, we consider a DDE modelling a semiconductor laser subject to external feedback.

Key words: Sensitivity to perturbation, transient response, phase-conjugate feedback laser

1 Introduction

The pseudospectrum of a matrix provides information about how its eigenvalues behave under arbitrary perturbations of a given size. This is particularly useful if the matrix under consideration models a physical system where parameters may be uncertain or may change under external perturbation. In particular, one would be interested in whether small perturbations to the system may cause an unwanted instability. Furthermore, the pseudospectrum gives a useful insight into the system's transient behaviour. If the system is

[1] Corresponding author.
Address: Bristol Laboratory for Advanced Dynamic Engineering, University of Bristol, Queen's Building, University Walk, Bristol BS8 1TR, UK
Email: kirk.green@bristol.ac.uk
Fax: +44 (0)117 954 6833
[2] Address: Bristol Laboratory for Advanced Dynamic Engineering, University of Bristol, Queen's Building, University Walk, Bristol BS8 1TR, UK

non-normal, that is, the eigenvectors of the system matrix are non-orthogonal, even a stable system can exhibit a large transient growth before eventual decay. In fact, this growth may be long lasted and may even be interpreted as an instability over a finite time interval. Furthermore, it is believed that this transient growth can lead to a trajectory of the system escaping the region of phase space where the linearisation is valid, nonlinear terms could then dominate, leading to instabilities [2,8,20].

Computing the pseudospectrum of a matrix is a classic problem [19]. This matrix (or linear operator) can, for instance, be obtained from the linearisation of a first-order system of nonlinear ordinary differential equations (ODEs) about some desired solution. The `Matlab` package `EIG-TOOL` [22] has been developed to visualise the pseudospectra of such systems. Furthermore, one may be interested in the behaviour of higher-order systems. Hence, methods have been developed to compute the pseudospectrum of polynomial eigenvalue problems (or matrix polynomials) [16,18,21].

In this paper we are interested in the pseudospectra of delay differential equations (DDEs). Found in many applications ranging from chemistry [7] and biology [3] to laser physics [10], the dynamics of systems modelled by DDEs is of great interest. Recently, computational techniques, once only available for the analysis of ODEs, have been developed for DDEs. These include numerical tools for bifurcation analysis, such as the `Matlab` package `DDE-BIFTOOL` [6], and techniques for manifold computations [11]. To this end, and to add to the numerical tools available for analysing DDEs, it is our aim to show how pseudospectra can be computed in systems modelled by DDEs. Two different notions of pseudospectra for DDEs are considered. Our main result deals with uncertainty in the governing system by computing pseudospectra with respect to perturbations applied to the individual system matrices. This is the natural approach when considering robust stability of solutions, and is related to the concept of stability radii [17]. On the other hand, if one is interested in analysing the transient behaviour of a DDE, in particular initial transient growth, the pseudospectra of the infinitesimal operator obtained via a discretisation of a continuous function over an entire delay interval must be considered. As an illustrative example we will consider a DDE modelling a semiconductor laser subject to phase-conjugate optical feedback (PCF) [10,12].

2 Delay differential equations

For readers less familiar with DDEs we first introduce some basic concepts; for further details see Refs. [5,13]. A DDE with multiple fixed discrete delays can be written as

$$\frac{dx(t)}{dt} = f(x(t), x(t-\tau_1), x(t-\tau_2), ..., , x(t-\tau_m), \eta) \tag{1}$$

where

$$f : \underbrace{\mathbb{R}^n \times \mathbb{R}^n \times \mathbb{R}^n \times ... \times \mathbb{R}^n}_{m+1 \text{ times}} \times \mathbb{R}^p \to \mathbb{R}^n$$

is autonomous and differentiable with respect to its arguments, and $\eta \in \mathbb{R}^p$ is a vector of parameters. The *phase space* of (1) is the infinite-dimensional space of continuous functions over the delay interval $[-\tau, 0]$ with values in $\mathbb{R}^n$, where τ is the maximal delay of (1). A *steady state* (or equilibrium) of (1) is a point x_0 such that $x_0(t) \equiv x_0$ solves (1) for all $t \in [-\tau, \infty)$ and fixed $x_0 \in \mathbb{R}^n$, $\eta^* \in \mathbb{R}^p$. In other words, $f(x_0, x_0, ..., x_0, \eta^*) = 0$.

The stability of x_0 can be obtained from the *variational equation*

$$\frac{dy(t)}{dt} = A_0(\underline{x}_0, \eta^*)y(t) + \sum_{i=1}^{m} A_i(\underline{x}_0, \eta^*)y(t-\tau_i) \tag{2}$$

which is the linearisation around $\underline{x}_0$, where $\underline{x}_0 = (x_0, x_0, ..., x_0)$, and the Jacobian matrices

$$A_0(\underline{x}_0, \eta^*) := \frac{\partial f}{\partial x(t)}(\underline{x}_0, \eta^*) \text{ and } A_i(\underline{x}_0, \eta^*) := \frac{\partial f}{\partial x(t-\tau_i)}(\underline{x}_0, \eta^*), \tag{3}$$

$i = 1, ..., m$.

When we define the $n \times n$ delayed characteristic matrix Δ as

$$\Delta(z) \equiv \Delta(\underline{x}_0, \eta^*, z) := zI - A_0(\underline{x}_0, \eta^*) - \sum_{i=1}^{m} A_i(\underline{x}_0, \eta^*) \exp(-\tau_i z) \tag{4}$$

then the eigenvalues are given as the roots of the *characteristic equation*

$$\det(\Delta(z)) = 0. \tag{5}$$

Equation (5) has infinitely many zeros. However, it is an important property of DDEs with fixed delays that the eigenvalues are discrete and that there are at most finitely many eigenvalues with real part larger than γ, for any fixed $\gamma \in \mathbb{R}$; see theorem 4.4 (i) of Ref. [5]. As for ODEs, a steady state is stable if there is no eigenvalue in the right-half of the complex plane.

Equation (2) can also be formulated as the abstract, non-delayed evolution equation on $X = C([-\tau, 0], \mathbb{C}^n)$:

$$\frac{dx_t}{dt} = \mathcal{A}x_t, \quad t \geq 0, \tag{6}$$

where $\mathcal{A}$ is the *infinitesimal generator* of (2), and $x_t \in D(\mathcal{A})$, such that

$$D(\mathcal{A}) := \left\{ \phi \in X \, : \, \dot{\phi} \in X, \, \dot{\phi}(0) = A_0\phi(0) + \sum_{i=1}^{m} A_i\phi(-\tau_i) \right\}. \tag{7}$$

Furthermore, the solutions of (2) and (6) are connected by $x_t(\theta) = x(t+\theta)$, $\theta \in [-\tau, 0]$, $t \geq 0$. The stability of (6) can be inferred by studying the eigenvalues of $\mathcal{A}$. These are identical to the solutions of (5).

3 Pseudospectra of the delayed characteristic matrix

In this section we are interested in the behaviour of solutions $z \in \mathbb{C}$ of the characteristic equation (5) under perturbations of the individual matrices A_i $(i = 0, ..., m)$. In terms of the DDE (1), this means that we consider perturbations to the vector field f. Let us therefore introduce perturbations

$$\widetilde{\Delta}(z) := B_0 + \sum_{i=1}^{m} B_i \exp(-\tau_i z) \tag{8}$$

and a vector of weights $(w_0, w_1, \ldots, w_m) \in \mathbb{R}^{m+1}$ with the weight $w_i \geq 0$ being associated to the perturbation B_i of A_i. Using this we define the ε-pseudospectra $\Lambda_\varepsilon(\Delta)$ of Δ as the set of complex numbers

$$\Lambda_\varepsilon(\Delta) := \left\{ z \in \mathbb{C} : \det\left(\Delta(z) + \widetilde{\Delta}(z)\right) = 0 \text{ for some } \widetilde{\Delta} \text{ with } \|B_i\| \leq \varepsilon w_i, \; i = 0, ..., m \right\}, \tag{9}$$

where $\|B_i\|$ denotes a general matrix norm of B_i.

Similar to the results for matrix polynomials, discussed in Ref. [18], the following theorem gives a computable formula for the ε-pseudospectra of Δ.

Theorem 1 *Let* $g(z) := w_0 + \sum_{i=1}^{m} w_i |\exp(-\tau_i z)|$, *and for* $\varepsilon > 0$

$$S := \left\{ z \in \mathbb{C} : \|\Delta(z)^{-1}\| \geq (\varepsilon g(z))^{-1} \right\}. \tag{10}$$

Then $\Lambda_\varepsilon(\Delta) = S$.

PROOF. The proof is similar to the one of Lemma 2.1 in Ref. [18]. We first show that $\Lambda_\varepsilon(\Delta) \subset S$. Let $z \in \Lambda_\varepsilon(\Delta)$ and assume that z is not an eigenvalue of Δ, since in this case the statement is trivial. If $\widetilde{\Delta}$ is chosen such that $\Delta(z) + \widetilde{\Delta}(z) = \Delta(z)\left[I + \Delta(z)^{-1}\widetilde{\Delta}(z)\right]$ is singular, then

$$1 \leq \|\Delta(z)^{-1}\widetilde{\Delta}(z)\| \leq \|\Delta(z)^{-1}\|\|\widetilde{\Delta}(z)\| \leq \|\Delta(z)^{-1}\| \left(\varepsilon w_0 + \sum_{i=1}^{m} \varepsilon w_i |\exp(-\tau_i z)|\right), \tag{11}$$

and thus $z \in S$, see (10).

To prove the converse statement, that is $S \subset \Lambda_\varepsilon(\Delta)$, choose $z \in S$ and assume again that z is not an eigenvalue of Δ, since otherwise nothing has to be proved. Choose y with $\|y\| = 1$ such that $\|\Delta(z)^{-1}y\| = \|\Delta(z)^{-1}\|$ and set $x := \Delta(z)^{-1}y/\|\Delta(z)^{-1}\|$. Then $\|x\| = 1$, and furthermore there exists a matrix H with $\|H\| = 1$ and $Hx = y$. We define $E = -H/\|\Delta(z)^{-1}\|$ and find that $(\Delta(z) + E)x = 0$, and therefore $\det(\Delta(z) + E) = 0$. In addition we obtain from (10)

$$\|E\| = 1/\|\Delta(z)^{-1}\| \leq \varepsilon g(z). \tag{12}$$

Now let us finally introduce

$$B_0 = \frac{w_0}{g(z)}\, E \quad \text{and} \quad B_i = \frac{|\exp(-\tau_i z)| w_i}{\exp(-\tau_i z) g(z)}\, E \quad \text{for } i = 1, \ldots, m. \tag{13}$$

Using (12) it is easy to check that $\|B_i\| \leq \varepsilon w_i$ for all i. Moreover,

$$B_0 + \sum_{i=1}^{m} B_i \exp(-\tau_i z) = E, \tag{14}$$

which proves $z \in \Lambda_\varepsilon(\Delta)$.

Furthermore, for a matrix $A \in \mathbb{C}^{n\times n}$ let $\sigma_{\min}(A)$ denote its smallest singular value. In the special case of using the 2-norm, (10) can be written as

Corollary 2 $\Lambda_\varepsilon(\Delta) = \{z \in \mathbb{C} : \sigma_{\min}(\Delta(z))/g(z) \leq \varepsilon\}$;

see Lemma 1.1 in Ref. [16].

To compute pseudospectra of (9) we use (10). In particular, when considering the 2-norm, we can utilise Corollary 2. Our method is standard [19]; we evaluate $(\|(\Delta(z))^{-1}\|\, g(z))^{-1}$ or, in the case of the 2-norm, $\sigma_{\min}(\Delta(z))/g(z)$ for values of z on a grid over the complex plane; to compute $\sigma_{\min}$ we use the `Matlab` function `svd`. The results are then plotted using a standard contour plotter, namely the `Matlab` function `contour`. For each pseudospectrum plot presented in Sec. 5 we used a 601×601 grid; computation time was 61.1 s on a 2.8 GHz `XEON` processor. Note that another algorithm to compute pseudospectra uses path following techniques to compute contours around the eigenvalues [16]. However, in the case of a DDE this method would prove highly inefficient due to the large number of eigenvalues present, particularly if the user wanted to compute the closed contours, for small ε, around every eigenvalue.

4 Pseudospectra of the infinitesimal generator

Transient behaviour has been shown to play an important role in the dynamics of systems with an ε-pseudospectrum which stretches into the right-half plane for small ε. Specifically, for a linear operator $\mathcal{L} : X \to X$, where X is a Banach space with norm $\|\cdot\|$, the ε-pseudospectrum is defined by

$$\Lambda_\varepsilon(\mathcal{L}) = \{z \in \mathbb{C} \,:\, z \in \Lambda(\mathcal{L}+\mathcal{E}) \text{ for some } \mathcal{E} \text{ with } \|\mathcal{E}\| \le \varepsilon\} \tag{15}$$

$$= \left\{ z \in \mathbb{C} \,:\, \|(zI-\mathcal{L})^{-1}\| \ge \frac{1}{\varepsilon} \right\}, \tag{16}$$

see Ref. [19] for details. It can be shown that if the ε-pseudospectrum extends into the right-half plane to $\Re(z) = \eta$, then a lower bound on the matrix exponential $\|e^{\mathcal{L}t}\|$ is given by η/ε [19]. If this initial growth is large, it is believed that a trajectory of a nonlinear system ($\dot{x} = \mathcal{L}x +$ h.o.t.) starting close to the steady state, may escape the basin of attraction and may be attracted to more complicated dynamics [8].

Information about the maximum transient growth of solutions of (2) and its equivalent (6) can be obtained by considering pseudospectra of the infinitesimal generator $\mathcal{A}$. In practice, we discretise $\mathcal{A}$ using the method described in Ref. [4]. The collocation scheme employed is based on an N-point Chebyshev method, over the delay interval $[-\tau, 0]$. This results in a matrix M of size $(N+1)n \times (N+1)n$. The pseudospectrum of M can then be computed using standard techniques. Specifically, we use (16) to evaluate $\|(zI-M)^{-1}\|_\infty$ on a grid over the complex plane. Note that the ∞-norm is consistent with

the maximum norm in $C([-\tau, 0], \mathbb{C}^n)$ and computationally cheaper than other alternatives.

5 Illustrative example: PCF laser

To illustrate our results, we consider the following, technologically relevant, example of a DDE modelling a PCF laser [9,15]

$$\begin{aligned}\frac{1}{\tau}\frac{dE}{dt} &= \frac{1}{2}\left[-i\alpha G_N(N(t) - N_{\text{sol}}) + \left(G(t) - \frac{1}{\tau_p}\right)\right] E(t) + \kappa E^*(t-1),\\ \frac{1}{\tau}\frac{dN}{dt} &= \frac{I}{q} - \frac{N(t)}{\tau_e} - G(t)\,|E(t)|^2,\end{aligned} \tag{17}$$

where the evolution of the complex electric field $E(t) = E_x(t) + iE_y(t) \in \mathbb{C}$ and the population inversion $N(t) \in \mathbb{R}$. Nonlinear gain is included in the term $G(t) = G_N(N(t) - N_0)(1 - \epsilon P(t))$ where $\epsilon = 3.57 \times 10^{-8}$ is the nonlinear gain coefficient and $P(t) = |E(t)|^2$ is the intensity. All other parameters were set to realistic values corresponding to a Ga-Al-As semiconductor laser, namely, $\alpha = 3$, $G_N = 1190\ \text{s}^{-1}$, $N_{\text{sol}} = 7.64 \times 10^8$, $N_0 = 1.64 \times 10^8$, $\tau_p = 1.4 \times 10^{-12}$ s, $\kappa = 4.2 \times 10^9\ \text{s}^{-1}$, $\tau = 6.667 \times 10^{-10}$ s, $I = 0.651$ A, $q = 1.6 \times 10^{-19}$ C, and $\tau_e = 2 \times 10^{-9}$ s [10,15].

For these parameter values, there exists a stable steady state solution given by

$$(E_x, E_y, N) = (1.8458, -0.24163, 7.6430). \tag{18}$$

This steady state was computed using `DDE-BIFTOOL` [6]. Note that, for numerical accuracy, we scale $E(t)$ by a factor of 10^{-2}, and $N(t)$ by a factor of 10^{-8}.

Linearisation of (17) around this steady state results in the following Jacobian matrices (see (2))

$$A_0 = \begin{pmatrix} -8.4982 \times 10^{-1} & 1.4790 \times 10^{-1} & 4.4373 \times 10^{1} \\ 3.7555 \times 10^{-3} & -2.8049 \times 10^{-1} & -2.2923 \times 10^{2} \\ -1.7537 \times 10^{-1} & 2.2958 \times 10^{-2} & -3.6079 \times 10^{-1} \end{pmatrix}, \tag{19}$$

and

$$A_1 = \begin{pmatrix} 2.80000 \times 10^{-1} & 0 & 0 \\ 0 & -2.80000 \times 10^{-1} & 0 \\ 0 & 0 & 0 \end{pmatrix}, \tag{20}$$

leading to the linearised system

$$\frac{dL}{dt} = A_0 x(t) + A_1 x(t-1). \tag{21}$$

where $x(t) = (E_x(t), E_y(t), N(t))$.

5.1 Computation of pseudospectra

Figure 1(a) shows the spectrum of the steady state (18) computed using `DDE-BIFTOOL` [6]. The spectrum has a characteristic shape with a *tail* of eigenvalues to the left, and a small number of eigenvalues to the right. The latter, upon variation of parameters, could possibly move into the right-half plane resulting in loss of stability of the steady state.

Figure 1(b) shows the ε-pseudospectrum computed using the method described in Sec. 3.1. Perturbations were weighted in the absolute sense, that is, $w_0 = w_1 = 1$ [18]. From rightmost to leftmost (or from outermost to innermost for closed curves), the contours correspond to pseudospectra with $\varepsilon = 1$, 10^{-1}, 10^{-2}, and 10^{-3}. It is clear that the real eigenvalue $\lambda_1 = -1.1864 \times 10^{-1}$ closest to the imaginary axis is most sensitive to perturbation, with the $\varepsilon = 10^{-2}$ contour reaching the right-half plane. However, it should be noted that the $\varepsilon = 10^{-2}$ contour surrounding the next two complex eigenvalues $\lambda_{2,3} = -8.3839 \times 10^{-1} \pm 3.5816i$ almost reaches the right-half plane. This latter observation could account for oscillatory behaviour in the transient or an instability to periodic motion of the steady state under small variations of parameters. Note that the eigenvalues to the left, those in the tail, are less sensitive to perturbation. Therefore, the eigenvalues which are likely to cross to the right-half plane under perturbation are those which are right-most, not those found in the tail. Furthermore, for large enough values of ε, the contours of the pseudospectrum do not close. In other words, under a large enough perturbation of the linearised system given (21), we may find eigenvalues in a large region of the left-half plane. Moreover, for small perturbations, we find a second $\varepsilon = 10^{-3}$ contour to the left in Fig. 1(b) which is unrelated to the rightmost tail of eigenvalues. We now examine these last observations.

Figures 1(c) to (f) show the result of applying random perturbations to the linearised system. Specifically, in each case we generated 500 normalised com-

plex perturbation matrices (P_0, P_1) with $\|P_j\| = \delta$, $j = 0, 1$. The 100 eigenvalues λ with greatest real part, of the perturbed characteristic equation $\lambda I - (A_0 + P_0) - (A_1 + P_1)\exp(-\lambda)$, were then computed using `DDE-BIFTOOL` [6] and the results plotted. Figures 1(c) to (f) show the results for $\delta = 1$, 10^{-1}, 10^{-2}, and 10^{-3}, respectively. In each case, the eigenvalues of the randomly perturbed characteristic equation are shown to lie within the corresponding ε-pseudospectrum contours of Fig. 1(b). Importantly, the eigenvalues for large values of δ, that is, $\delta = 1$ (Fig. 1(c)) and $\delta = 10^{-1}$ (Fig. 1(d)), are shown to cover a large area of the left-half plane. This confirms our result that the contours of the pseudospectrum do not close to the left, for a large enough perturbation. Note that for small values of δ, that is, $\delta = 10^{-3}$ (Fig. 1(f)), the rightmost perturbed eigenvalues are contained within the $\varepsilon = 10^{-3}$ pseudospectrum of the unperturbed characteristic which are closed curves centred on the eigenvalues shown in Fig. 1(a). However, one also observes perturbed eigenvalues to the left in Fig. 1(b). These correspond to the $\varepsilon = 10^{-3}$ contour and pose an interesting question: what eigenvalues of the unperturbed problem is this contour associated with? To answer this question we focus on a pair of normalised complex perturbation matrices P_j where $\|P_j\| = 10^{-3}$, $j = 0, 1$. Solutions of the characteristic matrix $\lambda I - (A_0 + B_0) - (A_1 + B_1)\exp(-\lambda)$ where $B_j = \mu P_j$ and a homotopy parameter $\mu \in [0, 1]$ were then computed. Specifically, we used

$$P_0 = \begin{pmatrix} -5.2808 \times 10^{-4} & -3.5322 \times 10^{-4} & -1.2306 \times 10^{-4} \\ 5.3584 \times 10^{-4} & -7.1252 \times 10^{-4} & -4.3189 \times 10^{-5} \\ 3.4686 \times 10^{-4} & -2.6639 \times 10^{-4} & -2.3613 \times 10^{-4} \end{pmatrix}, \tag{22}$$

and

$$P_1 = \begin{pmatrix} 3.4083 \times 10^{-4} & 4.0075 \times 10^{-4} & 3.7990 \times 10^{-4} \\ -3.2200 \times 10^{-4} & 2.0608 \times 10^{-4} & 4.7292 \times 10^{-4} \\ 5.7922 \times 10^{-4} & -4.8798 \times 10^{-4} & -5.5829 \times 10^{-4} \end{pmatrix}. \tag{23}$$

Figure 2 shows the results for a number of single computations where $\mu = \{10^{-12}, 10^{-11}, ..., 10^{0}\}$. The spectrum of each perturbed system consists of two tails: a rightmost tail, where the solutions are contained within the rightmost $\epsilon = 10^{-3}$ closed curve contours of Fig. 1(b), and a second tail to the left. In Fig. 2 the leftmost tail corresponds to $\mu = 10^{-12}$, the next tail to $\mu = 10^{-11}$, and so on, through to the tail corresponding to $\mu = 10^{0}$ at $\Re(z) \approx -10$. In other words, this second tail moves away from the imaginary axis as μ, that is, the size of the perturbation, is decreased. A comparison with the open contours of Fig. 1 leads us to believe that the second tail decreases without

bounds as μ goes to zero.

This behaviour can be explained by the fact that the original system (21) only contains delay terms in two of the three state variables. The perturbation B_1 introduces an additional delay term, which leads to the emergence of this second tail in the spectrum. However, it is important to note that this second tail exists to the left of the original tail, and that the main interest in computing pseudospectra, as defined in Section 3, lies in investigating the 'closeness to instability' of a system in which the second tail does not play a role.

This observed, non-physical phenomenon is due to the fact that general perturbations do not respect the structure of the original system. Similar problems arise in the linear analysis of higher-order ODEs. We mentioned earlier that pseudospectra of matrix polynomials have been defined for the analysis of higher-order ODEs using complex matrix polynomial perturbations that respect the higher-order structure. More recently, work in structured perturbations has been undertaken to provide a more accurate pseudospectra for ODEs [14,21]. It is hoped that this structured approach can be extended to DDEs in the future.

Figure 3 shows ε-pseudospectra where the perturbations are weighted differently in each case. Specifically, from Fig. 3(a) to (f) the weights (w_0, w_1) applied to the (A_0, A_1) matrices are $(0, 1)$, $(0.2, 0.8)$, $(0.4, 0.6)$, $(0.6, 0.4)$, $(0.8, 0.2)$, and $(1, 0)$, respectively. Again, from rightmost to leftmost (or from outermost to innermost for closed curves), the contours correspond to pseudospectra with $\varepsilon = 1$, 10^{-1}, 10^{-2}, and 10^{-3}. A common theme for all weightings is that the eigenvalues closest to the imaginary axis, not those in the tail, are most sensitive to perturbation. When the weight applied to the A_0 matrix (19) is increased (and the weight applied to the A_1 matrix (20) decreased), the eigenvalues closest to the imaginary axis become more sensitive to perturbation. At the same time, the eigenvalues in the tail become less sensitive to perturbation; see the extreme case of $(w_0, w_1) = (1, 0)$ shown in Fig. 3(f).

Figure 4(a) shows the pseudospectrum of the infinitesimal generator of the linearisation of (17) computed using the methods described in Section 4. Specifically, we used $N = 62$ Chebyshev points in the discretisation, resulting in a 189-dimensional linear system. Note that the number of Chebyshev points was chosen to ensure an accurate representation of the spectrum in the region of the complex plane considered in Figs. 1 and 3. From rightmost to leftmost (or from outermost to innermost for closed curves), the contours correspond to pseudospectrum with $\varepsilon = 1$, 10^{-1}, 10^{-2}, and 10^{-3} (the $\times$'s denote the spectrum). Note that these values of ε are not directly comparable to those in Fig. 1(b). The ε-pseudospectra contours in Fig. 4(a) can be used to give a lower bound on transient growth. The $\varepsilon = 10^{-1}$ contour is seen to stretch into the

right half plane to $\Re(z) = 3.4$, giving a lower bound on the transient growth of $\|e^{Mt}\|_\infty$ of 34; see Fig. 4(b). Finally, the time taken to compute Fig. 4(a) was 13483 s, that is, approximately 220 times the computational time taken to compute the pseudospectra shown in Figs. 1 and 3. This computational time may be reduced using the techniques described in Refs. [19,23]. These techniques are used in `EIG-TOOL`, where a similar pseudospectrum to that shown in Fig. 4(a) can be computed in 388 s. Note that the `EIG-TOOL` computation is based on a singular value decomposition and, hence, uses the 2-norm.

5.2 Nonlinear response

We now briefly investigate the effect of small perturbations to the steady state of the full nonlinear system (17). Figure 5 shows the time evolution (measured in units of the delay τ) of the light intensity $P(t) = |E(t)|^2$ of the PCF laser. To compute Fig. 5 we used a fourth order Adams-Bashforth integration scheme [1]. In Fig. 5(a) we started from an initial condition which is an increase of 0.15% above the steady state value (18), while Fig. 5(b) shows the result for an increase of 0.16%. Specifically, $(E_x(0), E_y(0), N(0)) = (1.8486, -0.24199, 7.6545)$ and $(E_x(0), E_y(0), N(0)) = (1.8488, -0.24202, 7.6552)$, respectively. In Fig. 5(a) the trajectory is seen to converge to the steady state (18) after an initial large transient growth, compare with Fig. 4(b). The same transient growth is seen in Fig. 5(b), however, this is now followed by attraction not to the steady state but to an attracting periodic solution [10]. Note that this periodic solution is also reached by starting from an initial condition which is a decrease of 0.4% below the steady state. It is believed that this instability is reached due to the initial, large transient growth in the trajectory.

6 Conclusions

Knowledge of the sensitivity of eigenvalues and the transient behaviour of a system is critical in providing robust stable operation. This is of particular importance when considering physical systems where parameters may be uncertain, or may change slightly during normal operation.

The computation of pseudospectra is one such technique that allows evaluation of the degree to which eigenvalues may be shifted under small perturbations of the governing equations of motion. We have presented two methods for the computation of pseudospectra in systems modelled by DDEs. Our main result allows for inexpensive computation of pseudospectra where perturbations applied to the 'instantaneous' and to the 'delay' Jacobian matrices of the

characteristic equation can be weighted independently. In the case of a single delay τ, time can be rescaled such that our method allows for perturbations in τ. Secondly, we studied the pseudospectrum of the infinitesimal operator. This approach allowed us to derive an estimate for the maximum transient growth. Hence, we have added to the numerical tools already available for the analysis of DDEs, allowing for a greater understanding of the dynamics of such systems.

For illustration, we considered the technologically relevant example of a DDE modelling a PCF laser. It was shown that the eigenvalues closest to the imaginary axis were most sensitive to perturbation. However, it was also shown that the pseudospectra was unbounded to the left of the complex plane. This was confirmed by applying random matrix perturbations of a known size to the unperturbed eigenvalue problem. We found this to be an effect of introducing an additional delay term not found in the unperturbed problem. Pseudospectra computed using our novel method were shown to be in qualitative agreement with pseudospectra of a linear operator obtained from the discretisation of the infinitesimal operator of the DDE. An interesting question is to what degree our inexpensive method may be used to provide information on the transient growth.

Finally, it was shown that trajectories starting close to the steady state of the full nonlinear system may escape its basin of attraction and be attracted to a more complicated solution. This is a consequence of the non-normality of the system, identified by the pseudospectra, and was shown to result in an instability to a periodic oscillation under small perturbation of initial conditions.

Acknowledgements

The authors would like to thank A. R. Champneys and M. I. Friswell for helpful comments on a draft version of this paper. This research was supported by the EPSRC grant GR/535684/01.

References

[1] M. Abramowitz and I. A. Stegun, editors, *Handbook of Mathematical Functions with Formulas, Graphs, and Mathematical Tables*, Dover Publications, 1974.

[2] J. S. Baggett, T. A. Driscoll, and L. N. Trefethen, A mostly linear model of transition to turbulence, *Physics of Fluids* **7** (1995) pp. 833–838.

[3] C. T. H. Baker, G. A. Bocharov, and F. A. Rihan, A report on the use of delay differential equations in numerical modelling in the biosciences, Technical Report 343, Department of Mathematics, University of Manchester, July 1999.

[4] A. Bellen and S. Maset, Numerical solution of constant coefficient linear delay differential equations as abstract cauchy problems, *Numer. Math.* **84** (2000) pp. 351–374.

[5] O. Diekmann, S. A. Van Gils, S. M. Verduyn Lunel, and H. O. Walther, *Delay Equations: Functional-, Complex-, and Nonlinear Analysis*, volume 110, Springer-Verlag, 1995.

[6] K. Engelborghs, T. Luzyanina, and G. Samaey, DDE-BIFTOOL v2.00: a Matlab package for bifurcation analysis of delay differential equations, Technical Report TW-330, Department of Computer Science, K. U. Leuven, Belgium, 2001, `http://www.cs.kuleuven.ac.be/~koen/delay/ddebiftool.shtml`.

[7] I. R. Epstein and J. A. Pojman, *An Introduction to Non-linear Chemical Oscillations*, Oxford University Press, New York, 1998.

[8] T. Gebhardt and S. Grossmann, Chaos transition despite linear stability, *Phys. Rev. E* **50** (1994) pp. 3705–3711.

[9] G. R. Gray, D. Huang, and G. P. Agrawal, Chaotic dynamics of semiconductor lasers with phase-conjugate feedback, *Phys. Rev. A* **49** (1994) pp. 2096–2105.

[10] K. Green and B. Krauskopf, Global bifurcations at the locking boundaries of a semiconductor laser with phase-conjugate feedback *Phys. Rev. E* **66** (2002) 016220.

[11] K. Green, B. Krauskopf, and K. Engelborghs, One-dimensional unstable eigenfunction and manifold computations in delay differential equations, *J. Comput. Phys.* **197** (2004) pp. 86–98.

[12] K. Green, B. Krauskopf, and G. Samaey, A two-parameter study of the locking region of a semiconductor laser subject to phase-conjugate feedback, *SIAM J. Dynamical Systems* **2** (2003) pp. 254–276.

[13] J. K. Hale and S. M. Verduyn Lunel, *Introduction to Functional Differential Equations*, Springer-Verlag, 1993.

[14] D. Hinrichsen and B. Kelb, Spectral value sets: a graphical tool for robustness analysis, *System and Control Letters*, **21** (1993) pp. 127–136.

[15] B. Krauskopf, G. R. Gray, and D. Lenstra, Semiconductor laser with phase-conjugate feedback: Dynamics and bifurcations, *Phys. Rev. E* **58** (1998) pp. 7190–7196.

[16] P. Lancaster and P. Psarrakos, On the pseudospectra of matrix polynomials, Technical Report 445, University of Manchester, 2004, `http://www.maths.man.ac.uk/~nareports/narep445.pdf`.

[17] M. Michiels, K. Green, T. Wagenknecht, and S.-I. Niculescu, Pseudospectra and stability radii for analytic matrix functions with application to time-delay systems, Technical Report TW-425, Department of Computer Science, K. U. Leuven, Belgium, 2005, `http://www.cs.kuleuven.ac.be/publicaties/rapporten/tw/TW425.abs.html`.

[18] F. Tisseur and N. J. Higham, Structured pseudospectra for polynomial eiegnvalue problems, with applications, *SIAM J. Matrix Anal. Appl.* **23** (2001) pp. 187–208.

[19] L. N. Trefethen, Computation of Pseudospectra, *Acta Numerica* (1999) pp. 1–46.

[20] L. N. Trefethen, A. E. Trefethen, S. C. Reddy, and T. A. Driscoll, Hydrodynamic stability without eigenvalues, *Science* **261** (1993) pp. 578–584.

[21] T. Wagenknecht and J. Agarwal, Structured pseudospectra in structural engineering, *International Journal for Numerical Methods in Engineering* (2005); to appear.

[22] T. G. Wright, *EIG-TOOL*, Oxford University, 2002, `http://www.comlab.ox.ac.uk/pseudospectra/eigtool/`.

[23] T. G. Wright and L. N. Trefethen, Large-scale computation of pseudospectra using arpack and eigs, *SIAM Journal on Scientific Computing* **23** (2001) pp. 591–605.

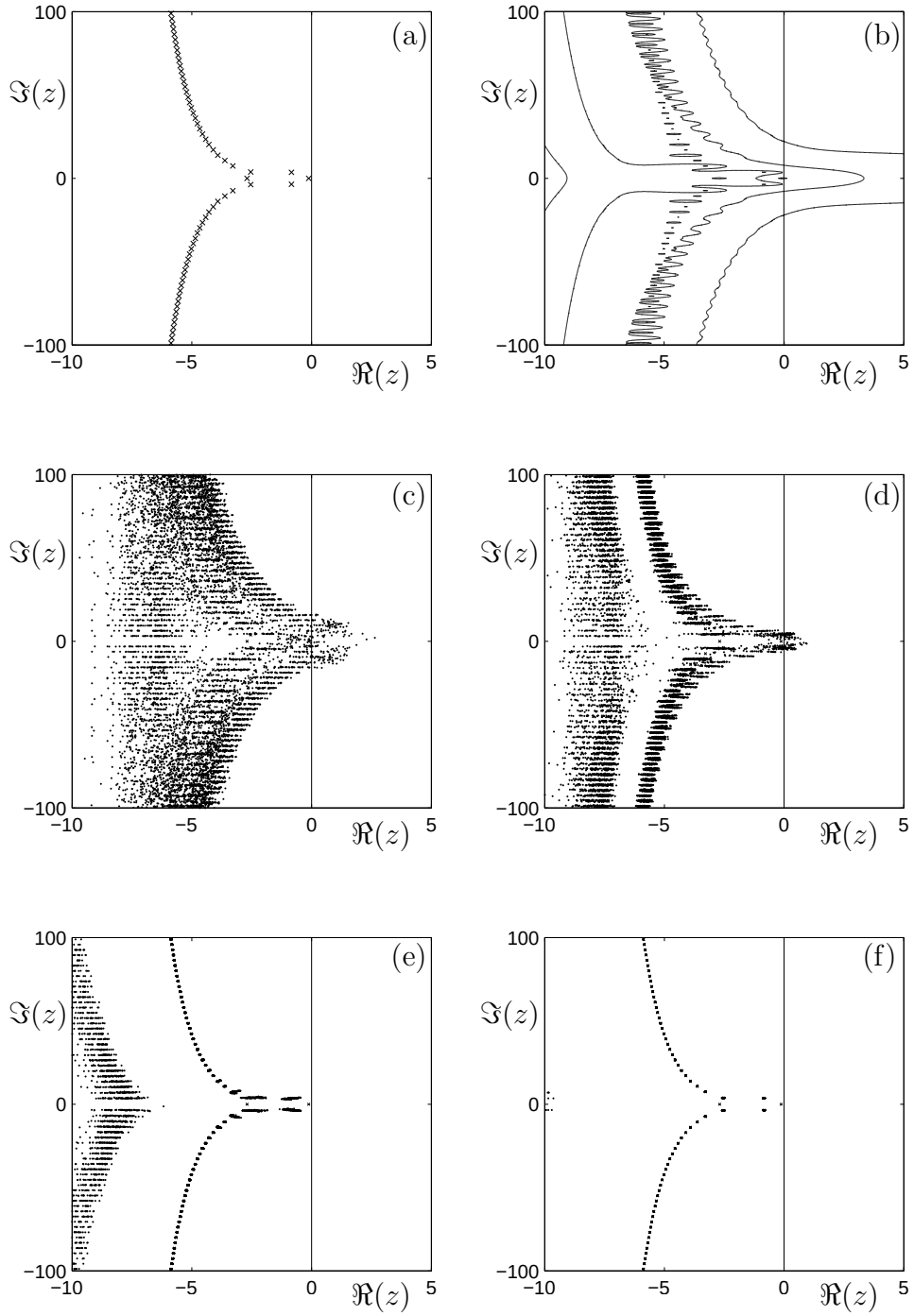

Fig. 1. Pseudospectrum of the DDE (17). Panel (a) shows the spectrum of the unperturbed problem computed using `DDE-BIFTOOL`. Panel (b) shows the ε-pseudospectrum where from rightmost to leftmost (or outermost to innermost for closed curves), the contours correspond to $\varepsilon = 1$, 10^{-1}, 10^{-2}, and 10^{-3}. Panels (c) to (f) show approximations of the ε-pseudospectrum where the eigenvalue problem was perturbed by random complex matrices of norm $\delta = 1$, 10^{-1}, 10^{-2}, and 10^{-3}, respectively.

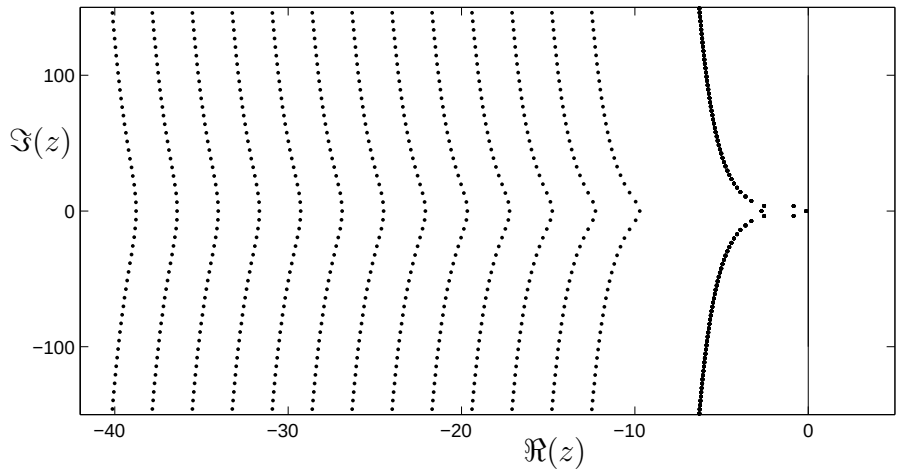

Fig. 2. Homotopy applied to random perturbation matrices $B_j = \mu P_j$, where $\|P_j\| = 10^{-3}$, $j = 0, 1$. From leftmost to rightmost, the tails for $\Re(z) < -10$ correspond to increased values of the homotopy parameter $\mu = 10^p$ where the integer $p = -12...0$, respectively.

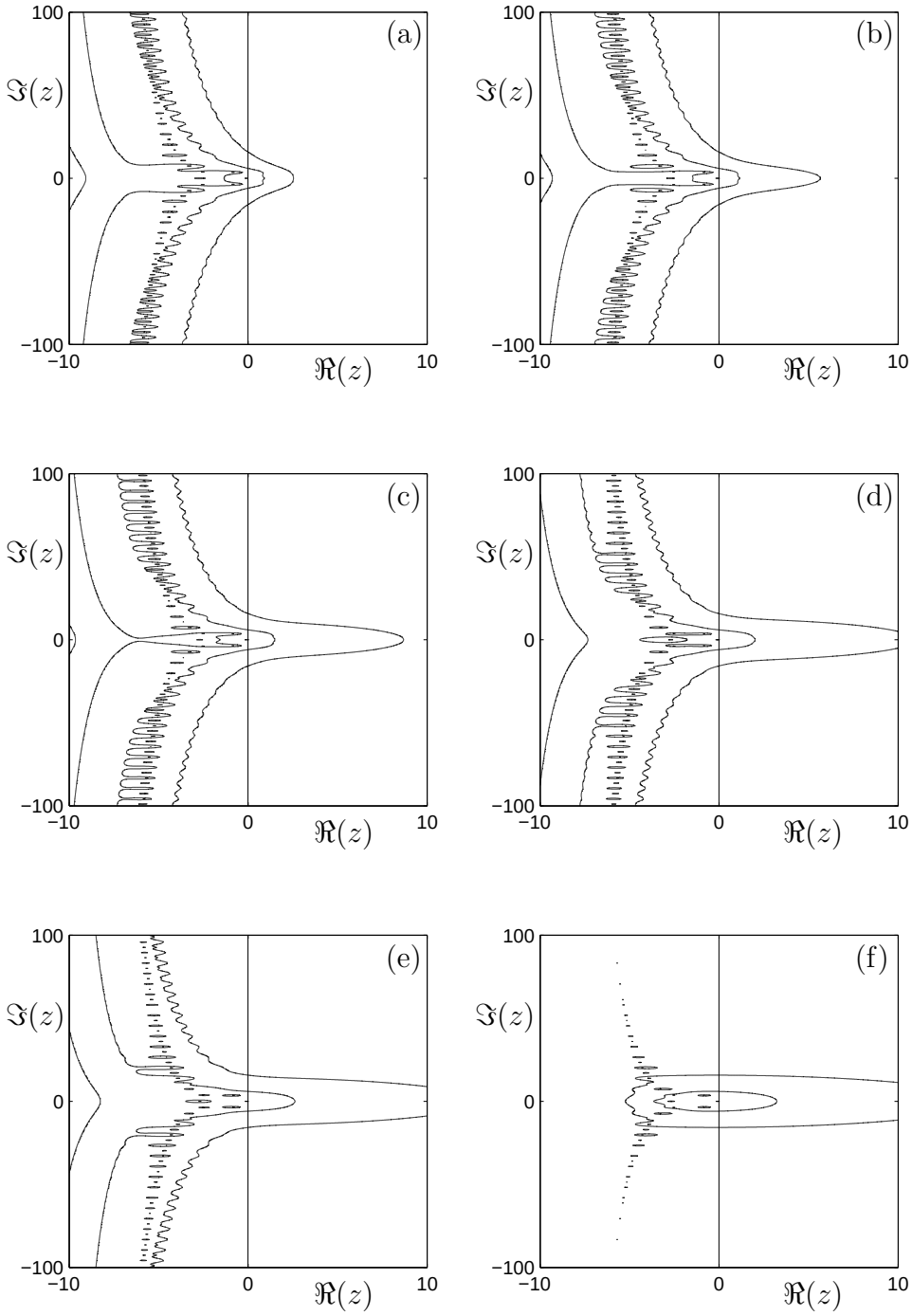

Fig. 3. Weighted pseudospectra of the DDE (17). In each panel, from rightmost to leftmost (or outermost to innermost for closed curves), the contours correspond to $\varepsilon = 1$, 10^{-1}, 10^{-2}, and 10^{-3}. From (a) to (f), the weights (w_0, w_1) applied to the (A_0, A_1) matrices were $(0, 1)$, $(0.2, 0.8)$, $(0.4, 0.6)$, $(0.6, 0.4)$, $(0.8, 0.2)$, and $(1, 0)$, respectively.

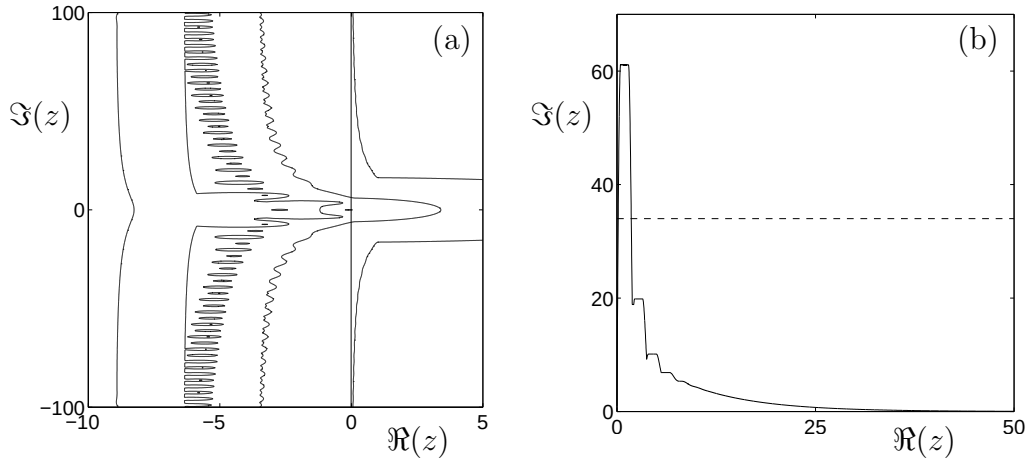

Fig. 4. Pseudospectra of the discretisation M of the infinitesimal generator $\mathcal{A}$ given by (6) (a). Time evolution of the matrix exponential $\|e^{Mt}\|_\infty$ (b); the dashed line showing the lower bound on the maximum transient growth as given by (a).

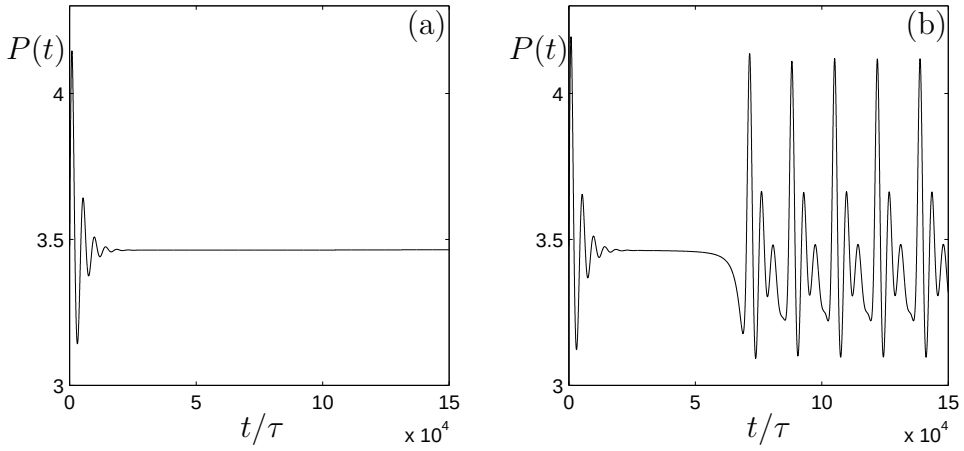

Fig. 5. Simulation of the full nonlinear DDE (17). Panels (a) and (b) show the dynamics after small perturbations to the steady state (18) by increases of 0.15% and by a 0.16%, respectively.